

## Article

# Effect of Electrodeposited Gold Coatings on Micro-Gaps, Surface Profile and Bacterial Leakage of Cast UCLA Abutments Attached to External Hexagon Dental Implants

Terry R. Walton

School of Dentistry, Faculty of Medicine and Health, University of Sydney, Sydney, NSW 2006, Australia; terry.walton@sydney.edu.au

**Abstract: Purpose:** The objective of the study was to qualitatively assess the micro-gap dimensions, connecting fitting surface profile, and bacterial leakage of cast high-gold-alloy UCLA abutments, with or without electrodeposited gold coatings attached to external hexagon implants. **Materials and methods:** Sixteen plastic UCLAs (PUCLAs) were cast with a high-gold-content alloy. Eight were electrolytically gold plated. Five machined cast-to-UCLA (GUCLA) control abutments were cast with the same alloy. All abutments were attached to external hexagon implants, giving 21 implant-abutment combinations (IACs). External perimeter micro-gaps measured with SEM under shadow eliminating silhouette illumination and 2000× magnification were averaged over three regions. The IACs were examined for *E. coli* leakage following an initial sterility test. Disassembled combinations were examined with SEM, and surface profiles were qualitatively assessed. **Results:** External micro-gap measurements did not reflect the variable connecting surface profiles, but average values < 5.0 μm were observed for all IACs measured under the shadow eliminating silhouette illumination for both cast and pre-machined external hexagon abutments with and without Au plating. *E. coli* transfer was observed in 3 of 5 PUCLA-plated and 2 of 5 PUCLA-non-plated IACs. No transfer occurred in the 3 GUCLA-non-plated or 2 GUCLA-plated control IACs. Abutment connecting surfaces, both Au-plated and not Au-plated, showed plastic deformation (smearing) in variable mosaic patterns across the micro-gap. **Conclusions:** Micro-gap dimensions < 5 μm were obtained with both the high noble metal cast and pre-machined control external hexagon abutments with and without Au electrodeposited on the abutment connecting surface. Regions of intimate contact due to plastic deformation (smearing) of these surfaces were observed. A continuous smeared region around the circumference of the surfaces can provide an effective barrier to the egress of *E. coli* bacteria from the internal regions of the implant under static loading. The sample size was insufficient to determine if the gold coating resulted in a superior bacterial barrier.



**Citation:** Walton, T.R. Effect of Electrodeposited Gold Coatings on Micro-Gaps, Surface Profile and Bacterial Leakage of Cast UCLA Abutments Attached to External Hexagon Dental Implants. *Coatings* **2023**, *13*, 1976. <https://doi.org/10.3390/coatings13121976>

Academic Editors: Egemen Avcu, Yasemin Yildiran Avcu and Mert Guney

Received: 29 October 2023

Revised: 17 November 2023

Accepted: 18 November 2023

Published: 21 November 2023



**Copyright:** © 2023 by the author. Licensee MDPI, Basel, Switzerland. This article is an open access article distributed under the terms and conditions of the Creative Commons Attribution (CC BY) license (<https://creativecommons.org/licenses/by/4.0/>).

**Keywords:** external-hexagon implants; implant-abutment connections; electrolytic deposition; micro-gap; SEM; bacterial leakage

## 1. Introduction

The long-term success of osseointegrated implant dentistry depends on the ongoing biological and biomechanical integrity of the bone/implant, implant/abutment, and abutment/prosthesis interfaces. Factors specifically affecting the implant/abutment integrity include the material composition, approximation of the components (fit), interface geometry and design, and connection screw mechanics [1].

Irrespective of the composition, geometry, and approximation of the implant and abutment, there is always a “micro-gap” between the two. This occurs due to small asperities in the fitting surfaces of the implants and abutments, preventing a “perfect” surface approximation. Micro-gaps are mostly measured at the external perimeter of the implant/abutment connection. There is some controversy concerning the dimensions of

these measurements relative to implant geometry. An assessment of 13 commercially available implant systems in 1997 indicated micro-gaps were on average  $<10\ \mu\text{m}$  [2]. In a recent study in 2020, micro-gaps of both internal and external machined connections were smaller than generally expected and ranged from 0.5 to 2.5  $\mu\text{m}$  [3]. It is possible that more precise current machining techniques account for this improved accuracy. It is generally accepted that machined surfaces will result in smaller micro-gaps than cast surfaces [4,5], although this has been refuted [6]. It has also been claimed that external perimeter measurements of micro-gaps have overestimated their influence. It was suggested that the pathway for bacteria to ingress into the micro-gaps is complex due to some regions being in direct contact and providing a sinuous and possibly continuous barrier across the implant/abutment interface [7]. Tissue-level implants avoid this pathway for bacterial contamination through the micro-gap by having the abutment/prosthesis connection above the mucosal cuff [8]. However, aesthetic complications limit the use of these implants to posterior regions in single-tooth and partial edentulous replacements.

The micro-gap at the implant/abutment connection in “bone-level” implants allows bacteria from the screw channel to transverse through the gap and also facilitates a reservoir for bacteria entering from the surrounding mucosal sulcus. This contamination directly from bacteria, or their endotoxins, is claimed to result in a 360-degree zone of inflammation contributing to horizontal and vertical bone loss [9], the degree of which is claimed to be dependent on the geometry/design of the implant and abutment and the position of the micro-gap relative to the crestal or marginal bone level (MBL) [10]. The more coronal the placement of the micro-gap relative to MBL, the less vertical bone loss [11]. The larger the dimension of the micro-gap, the greater the bone loss [12].

It has also been shown that MBL is influenced by micromovements at the implant/abutment junction during function [10,12]. It is postulated that these movements “pump” bacteria into the surrounding tissues. It is accepted that the smaller the implant/abutment misfit (micro-gap) and the more stable the joint, the less bacterial contamination will occur [13].

An alternative explanation for marginal bone loss is that tribocorrosion products arising from simultaneous chemical, wear, and electrochemical interactions are released and penetrate the surrounding tissues, resulting in osteolytic changes. This is referred to as a foreign body reaction [14,15]. The degree of tribocorrosion will be influenced by the composition of the components, the degree of misfit, and the stability of the joint during function.

Screws provide the implant/abutment connection. The rotational force draws the connecting surfaces together and is maintained by the degree of tension or preload developed [16]. Surface coating of screws with materials such as teflon or gold, which undergo some plastic deformation, helps to maintain this preload and prevent screw loosening during function. In addition, the greater the contacting implant/abutment surfaces, that is, the better the fit, the less “settling” (plastic deformation of surface asperities) will occur between the components during loading and the longer the preload, and therefore joint stability, will be maintained [16]. The greater the torque, the higher the preload and greater the reduction in micro-gap dimensions [3,17]. Excessive torque, however, can result in a screw fracture.

It is generally promoted that external hexagon implants with matched abutment diameters will be associated with an inevitable 1.0–1.5 mm vertical bone loss, as evidenced by a 2-dimensional radiographic examination after the first year of loading [18]. Other studies, however, dispute this claim. In an up-to-14-year study of single implant-supported crowns (SICs), 34% did not demonstrate bone loss to the first thread (0.6 mm) of the external hexagon implants with matched abutment profiles over the study period [19].

The results in the above-cited up-to-14-year study are contrary to accepted outcomes in several other ways, in addition to the documented MBLs. The implant/abutment design was hexagonal with matched external diameters; the University of California at Los Angeles (UCLA) abutments were cast; screw loosening incidence was relatively low (2.3%); and the incidence of peri-implantitis defined by bone loss  $>2\ \text{mm}$  subsequent to loading was low

(0.5%). The only modification to the commonly undertaken fabrication protocols was that the abutment fitting surfaces were electrolytically gold-plated [19].

It has been subsequently demonstrated that an elemental electrodeposited gold coating lowered titanium ion release but increased Au ion release into the surrounding medium in an in vitro dynamic accelerated aging study [20]. Osteolytic effects of titanium in tissues have been documented [21,22]. Contrarily, Au ions have been shown to have antibacterial and anti-inflammatory effects on surrounding tissues [23,24].

It was also postulated that the gold coating provided an enhanced surface approximation (seal), thus reducing the micro-gap dimension and resultant bacterial contamination [19]. In addition, it possibly increased surface area contact and frictional adherence between the approximating implant/abutment surfaces through plastic deformation of the highly ductile elemental gold. Thus, screw preload would be enhanced without increasing screw torque above recommended levels; joint stability would be increased; and the incidence of screw loosening would be reduced. It has been shown that electroplated gold thickness is linearly related to the plating time [25]. Further research is indicated.

The aims of this study were: 1. Qualitatively examine using scanning electron microscopy (SEM) with variable illumination and magnification, micro-gap dimensions, and the interface connecting the surface profile of cast UCLA high-gold content alloy abutments attached to external hexagon implants with and without an electrodeposited gold coating. The null hypothesis was that there was no difference between cast UCLA abutments with and without an electrodeposited gold coating.

2. Assess the bacterial leakage at these implant-abutment assemblies.

The second null hypothesis was that there was no difference in bacterial leakage between the cast abutments with or without an electrodeposited gold coating.

## 2. Materials and Methods

### 2.1. Abutment Preparation

Sixteen plastic UCLA abutments (PUCLA) designed to fit external hexagon implants (Biomet 3i™, Miami, FL, USA) were cast with a high gold content alloy (V classic; Cendres + Métaux SA, Biel, Switzerland) in a commercial laboratory (Wallis Franklin Ceramist, Sydney, Australia) (Table 1). Five machined cast-to-UCLA abutments (NobelBiocare, Zurich, Switzerland) (GUCLA) were also cast with the same gold alloy to act as controls to ensure the protocols used in the commercial laboratory resulted in micro-gaps comparable with those reported in the literature for machined abutments [3,4]. The implant fitting surfaces were sand blasted with 120-grit aluminum oxide powder (Alphabond Dental Willoughby, Sydney, Australia) with a pen-nozzle sand blaster at 4.0 bar (Caswell, Hoppers Crossing, Australia). Eight of the PUCLA and 2 of the GUCLA abutments were then immersed in a plating bath (Auroplatmini; Wieland Edelmetalle GmbH, Pforzheim, Germany) filled with a plating solution (Aurogold C5 1.5 gAu/L; Alphabond Dental Pty Ltd., Roseville, Australia) for 2 h with a current of 2.8 V. The plating conditions resulted in a Au-deposited layer of approximately 200 nm [25]. These plated abutments were designated PUCLA-P (n = 8) and GUCLA-P (n = 2). The remaining non-plated samples were designated PUCLA-N (n = 8) and GUCLA-N (n = 3) (Figure 1).

The 21 abutments were attached to regular platform (3.75 mm) external hexagon implants (NobelBiocare, Zurich, Switzerland) held in a bench-mounted vice and torqued to 32 Ncm<sup>2</sup> with sustained tension for 20 s. Gold-plated stainless steel screws (Biomet 3i™, Miami, FL, USA) were used for the castable abutments, and teflon-coated titanium screws (Nobel Biocare, Zurich, Switzerland) were used for the cast-to abutments as recommended by the manufacturer. Thus, 21 implant-abutment combinations (IACs) were prepared.

**Table 1.** Composition of the gold alloy—V classic.

Element	Composition %
Gold—Au	75
Palladium—Pd	19
Silver—Ag	1
Copper—Cu	0.44
Zinc—Zn	0.5
Tin—Sn	2
Indium	2
Iridium—Ir	0.01
Ruthenium—Ru	0.06

**Figure 1.** Samples of the PUCLA abutments (N = non-plated, P = plated).

### 2.2. SEM Evaluation of External Perimeter Micro-Gaps

The width of the micro-gap between the implants and abutments at the external perimeter was viewed at several magnifications and under different illumination conditions by SEM (Supra 40VP system, Oxford Instruments, Abingdon, UK).

Micro-gap measurements were obtained at 2000× magnification by first using a measurement cursor to demarcate the implant surface in the viewed external perimeter region. The cursor was then moved vertically to delineate the separation distance across the region. Variations in the abutment surface profile made it difficult to determine a precise gap, so the cursor was “averaged” midway between the high and low profiles. This “average” vertical separation—cursor height—was considered the gap width for that particular region.

The micro-gaps were measured, as described, in  $\mu\text{m}$  at 3 sites around the external perimeter, and mean micro-gaps were obtained.

### 2.3. Micro-Gap Leakage Test

The 21 IACs were placed in an ultrasonic bath (Coltene Whaledent: Altstätten, Switzerland) for 5 min and individually sealed in plastic sleeves. The sealed sleeves were then sterilized in an autoclave (Lisa: Bürmoos, Austria).

Five  $\mu\text{L}$  of bacterial suspension of *Escherichia Coli*—ATCC 25922 (*E. coli*) was introduced to the screw access channel of the abutments under sterile conditions. Sterilized rubber tubes were then pushed down onto the outside of the abutments, but short of the IAC, and 1 mL syringes were attached to the other end of the rubber tube to form the test assembly (TA) (Figure 2).

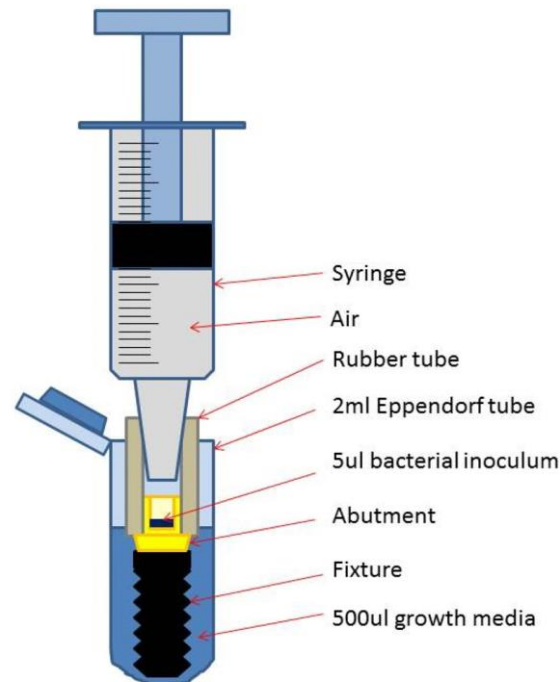


**Figure 2.** Schematic drawing of a test assembly (TA) placed in the Eppendorf tube with added growth medium.

A primary sterility test to ascertain if any contamination occurred during the tube and syringe connections was performed. Under sterile conditions, each TA was placed in 2 mL Eppendorf tubes (Hamberg, Germany), and 500  $\mu\text{L}$  of growth medium (brain heart infusion medium [3.7 g BHI/I i.e., 3.7%] supplemented with 1% glucose) (Sugstratlab; Sahlgrenska Hospital) was added to submerge the IACs above the micro-gap (Figure 2). After 10 min, the TAs were removed and the growth medium in the tubes incubated overnight at 37 degrees (sterility samples). They were then examined for turbidity.

The TAs that passed the initial sterility test were then transferred to new identical Eppendorf tubes, and another 500  $\mu\text{L}$  of the same growth medium was added. The air-filled syringe piston was then pressed half-way down (0.5 mL), corresponding to 1 bar air pressure, to assess bacterial leakage through the micro-gap into the surrounding growth medium. The connections were carefully observed during this press-down procedure to detect any liquid or bubbles passing into the growth medium. The piston was then fixed with adhesive tape to keep the pressure applied for 30 min. A sample of 20  $\mu\text{L}$  of the growth medium was serially diluted and spread on agar, and the remainder of the medium (50 + 430  $\mu\text{L}$ ) was spread on agar directly. Cultures were grown overnight aerobically at 37° in the growth medium and observed for colonization (present/absent).

A flow chart showing preparation and allocation of the 21 TAs is shown in Figure 3.

The IACs from the 2 test and 2 control groups were then disassembled, and the abutment, implant, and screw head fitting surfaces were imaged under SEM for a qualitative assessment.

The limited sample size precluded a quantitative statistical analysis.

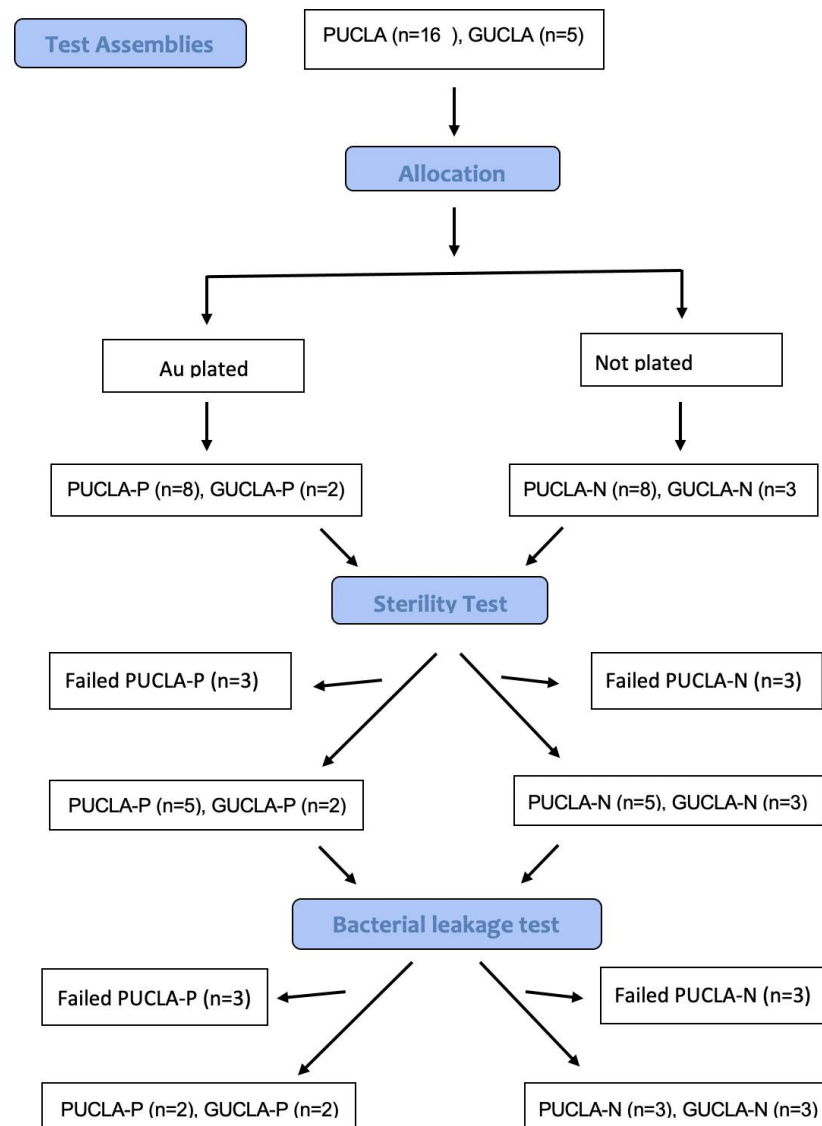


**Figure 3.** Flow chart showing allocation and bacterial leakage of the 21 TAs.

### 3. Results

#### 3.1. SEM Evaluation of External Perimeter Micro-Gaps

Quantitative assessment was difficult due to the beveled margin of both the implant and abutment and variable surface profile, resulting in shadowing and potential measurement error (Figures 4 and 5).

The most realistic assessment of the micro-gaps was achieved when the SEM imaging was performed with “silhouette” illumination, as this reduced any shadowing and facilitated assessment some depth into the micro-gap (Figure 5).

Figure 5 clearly demonstrates the difficulty in picking an actual micro-gap width due to both shadowing and variation in profile. One possible average gap width under normal illumination (Figure 5A) was 10  $\mu\text{m}$ . However, under silhouette illumination (Figure 5B), the same region could be assessed as having an average gap width of 3  $\mu\text{m}$ . Surface asperities near the outer rim of the abutment show intimate contact (0  $\mu\text{m}$  gap) with the implant surface in some regions. Adjacent regions can show variable gaps. Thus, these external micro-gap measurements are somewhat subjective due to the less than perfect flatness of the abutting surfaces, but the silhouette illumination gave a more realistic evaluation.

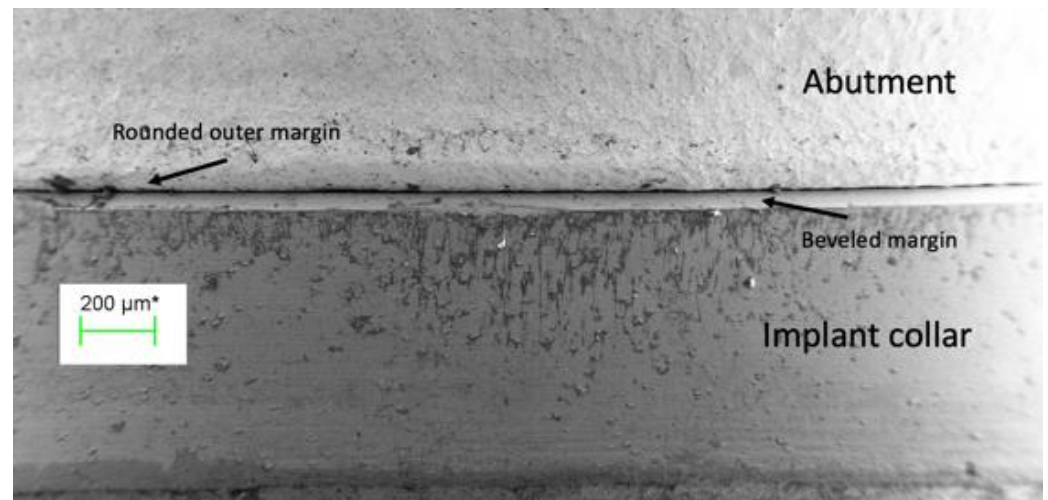


**Figure 4.** The external perimeter of the implant/abutment junction at 100 times magnification, illustrating the beveled margin on the implant and the rounded outer edge of the abutment. The bounded green line in the box is a linear reference of the magnification scale.

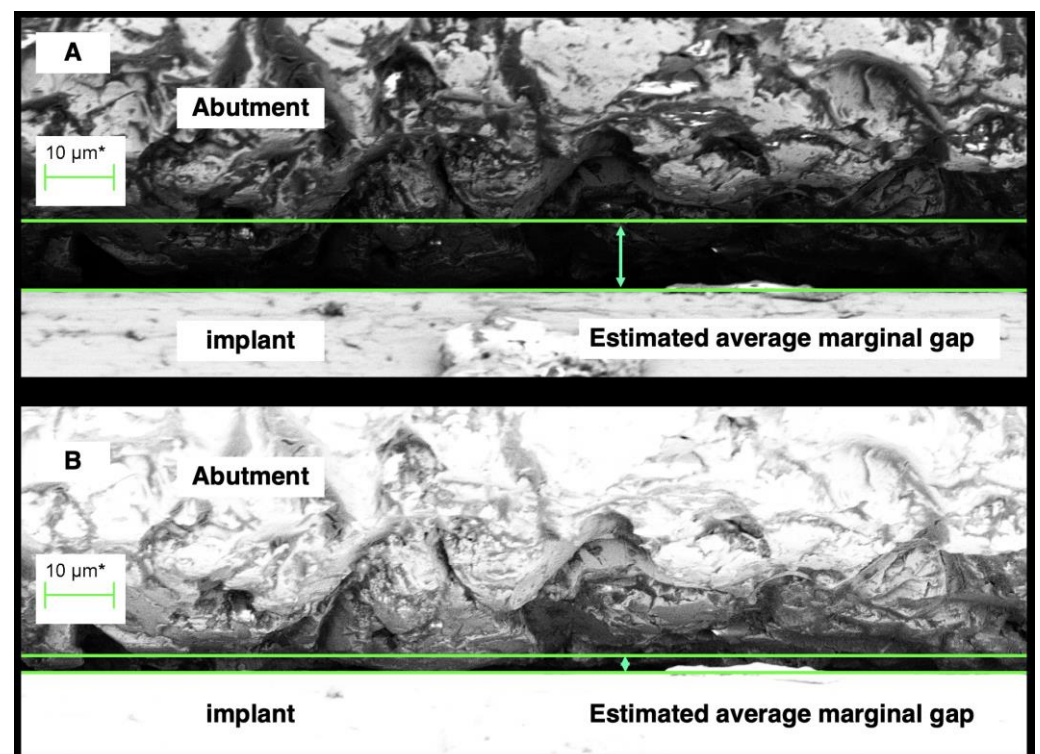


**Figure 5.** A region of the external perimeter of a micro-gap at 2000 times magnification. The distance between the green lines—the cursor height indicated by the green arrows, is considered the micro-gap width for the region. (A) shows assessment under normal illumination, while (B) shows assessment of the same region under silhouette illumination. The difference in actual gap width is significant, with the measurement at (B) more indicative of actual discrepancy of fit. The bounded green lines in the boxes in this and subsequent SEMs are a linear representation of the magnification scale.

Measurements of the external perimeter micro-gaps ( $\mu\text{m}$ ) of 4 of the PUCLA-plated IACs can be seen in Table 2. The mean micro-gaps over the three regions of all IACs were  $\leq 3.1 \mu\text{m}$ , and many regions were less  $< 2.0 \mu\text{m}$ .

**Table 2.** Measurements of the micro-gaps (MG) ( $\mu\text{m}$ ) of 4 of the PUCLA-P IACs.

TA	Description	MG-1	MG-2	MG-3	Mean MG
1	PUCLA-P1	3.2	3.2	2.9	3.1
2	PUCLA-P2	4.7	2.9	1.8	3.1
3	PUCLA-P3	1.7	1.4	2.5	2.5
4	PUCLA-P4	1.9	1.0	1.3	1.3

The average micro-gap profile and measurement of one region of each of the IACs in the two test and two control groups are depicted in Figure 6. There is little difference between the 4 groups. The variability of the profiles at these external perimeter sites is evident. The mean micro-gaps of the TAs in the cast-to (control) groups were within those published and indicated that the protocols used by the commercial laboratory were appropriate and at the desired standard.

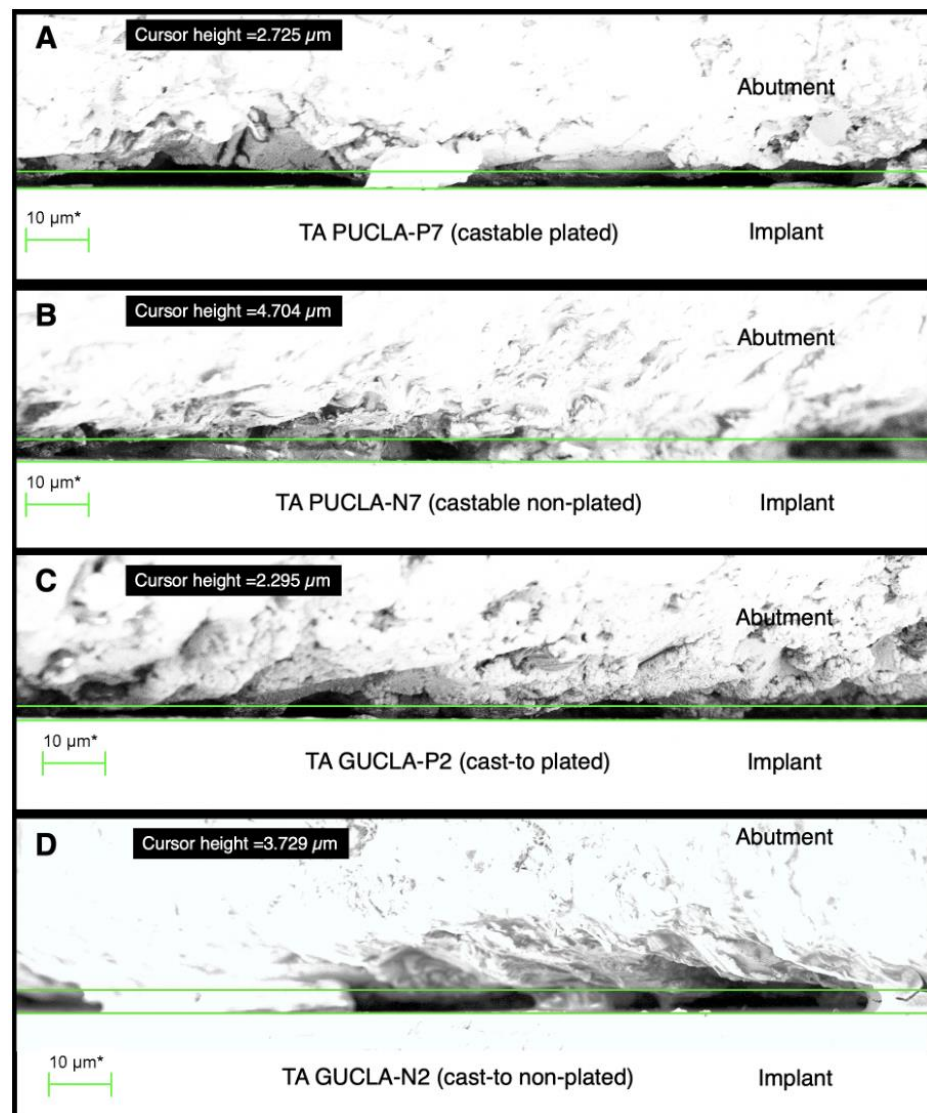


**Figure 6.** Sections of external perimeter micro-gap profiles for examples of the 4 different TA types: (A)—PUCLA-P7, (B)—PUCLA-N7, (C)—GUCLA-P2, (D)—GUCLA-N2. Note the surface asperities, which are in intimate contact with the implant surface. The average “gap” set by the cursor is  $<5 \mu\text{m}$  for the 4 TAs.

### 3.2. Micro-Gap Leakage Test

The primary sterility test proved effective in ascertaining if any bacterial inoculation of the growth medium occurred solely via transfer from the inoculated screw access shaft across the micro-gap.

Air leakage via the rubber tubes was identified by the immediate appearance of air bubbles in the immersed liquid growth medium when pressure was applied to the syringe in PUCLA-N TAs 1 and 2. These two TAs also failed the sterility test and were not included in the culture assessments. Bubbles also appeared after some time in two other TAs (PUCLA-P1, PUCLA-P5). Therefore, leakage of bacteria into the growth medium from sources other than the microgap could not be excluded, even though these assemblies passed the sterility test. Bubbles appeared after some time in the PUCLA-N4 TA. Even though the exchanged culture medium passed the sterility test and there was no transfer of bacteria via the micro-gap during the leakage assessment, this TA was also excluded from the culture assessments.

Therefore, 5 PUCLA-P TAs and 5 PUCLA-N TAs, as well as the 5 cast-to-UCLA (GUCLA) TAs (3 non-plated and 2 plated), were assessed for bacterial transfer across the micro-gap (Table 3). Bacterial transfer was observed in 3 of the PUCLA-P TAs and 2 of the PUCLA-N TAs. No bacterial transfer was observed in the 5 GUCLA control TAs. The sample size was not sufficient to support a statistical assessment of these qualitative observations.

**Table 3.** Colony-forming unit counts (CFUs) from the bacterial leakage test for the fifteen study TAs that passed the initial sterility test.

TA	Media/Dilution					Bubbles	Mean Microgap $\mu\text{m}$
	430 $\mu\text{L}$	50 $\mu\text{L}$	1:100	1:1000	1:10,000		
PUCLA-P2	~600	188	40	7	1	No	3.1
PUCLA-P3	~350	206	17	1	0	No	2.5
PUCLA-P4	~350	152	24	1	0	No	1.3
PUCLA-P6	0	-	-	-	-	No	2.8
PUCLA-P7	0	-	-	-	-	No	1.7
PUCLA-N3	xxx	xx	295	81	9	No	3.7
PUCLA-N5	0	-	-	-	-	No	4.6
PUCLA-N6	0	-	-	-	-	No	3.5
PUCLA-N7	0	-	-	-	-	No	4.7
PUCLA-N8	xxx	xxx	xxx	~500	80	Yes	4.9
GUCLA-N1	0	-	-	-	-	No	3.8
GUCLA-N2	0	-	-	-	-	No	4.1
GUCLA-N3	0	-	-	-	-	No	2.9
GUCLA-P1	0	-	-	-	-	No	3.0
GUCLA-P2	0	-	-	-	-	No	3.2

xxx = very thick, overlapping colonies. xx = Distinguishable CFUs but too many to count; - = not measured.

### 3.3. SEM Qualitative Assessment of Connecting Surface Profiles

An SEM image at 70 times magnification of the abutment screw seat of TA PUCLA-N5, which showed no *E. coli* leakage, is shown in Figure 7A. The higher magnification of part of this screw seat (454 $\times$ ) in Figure 7B shows a “smeared” surface, indicating an intimate approximation of the surfaces in the region.

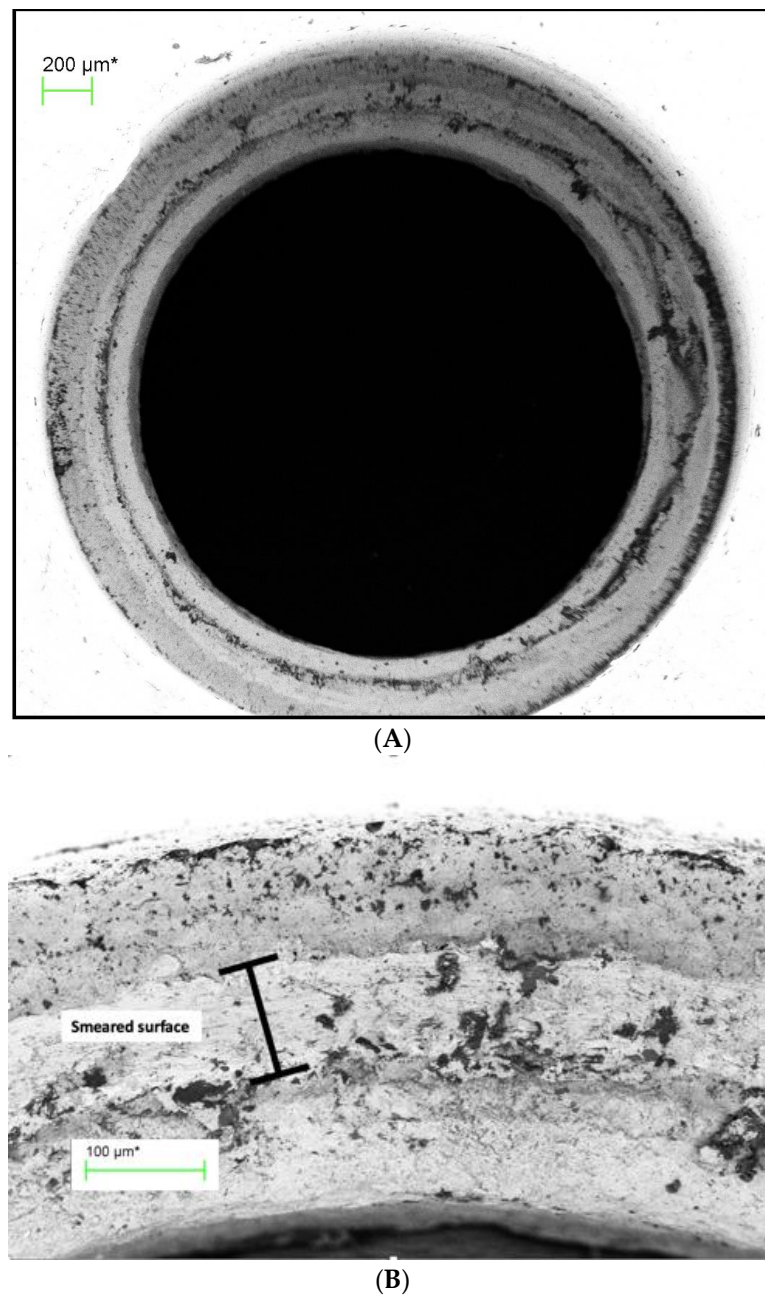
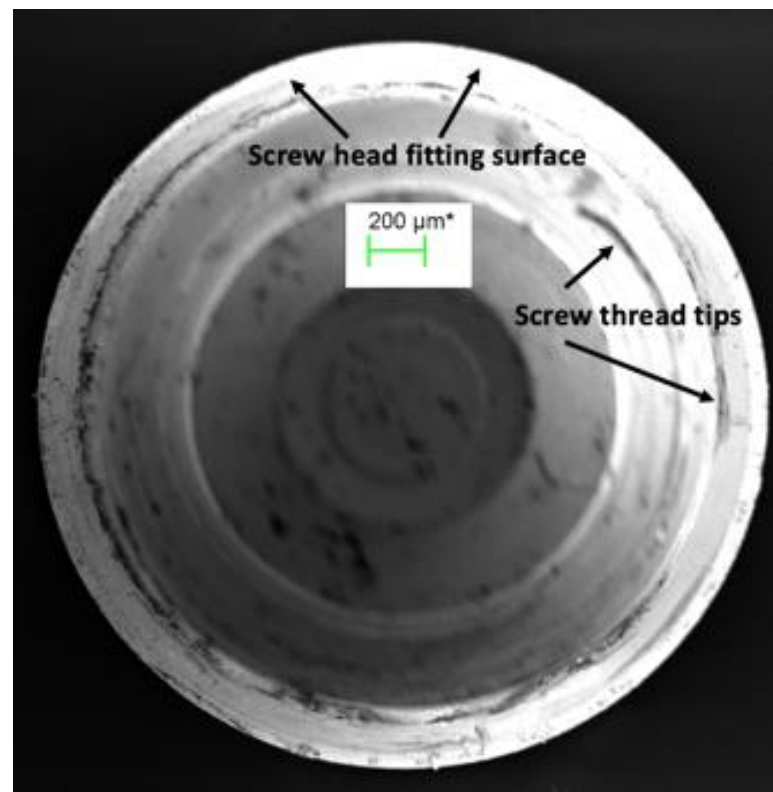


**Figure 7.** (A) Abutment screw seat of TA PUCLA-N5 (70×). (B) Higher magnification (454×) of a section of the screw seat of the abutment of TA PUCLA-N5.

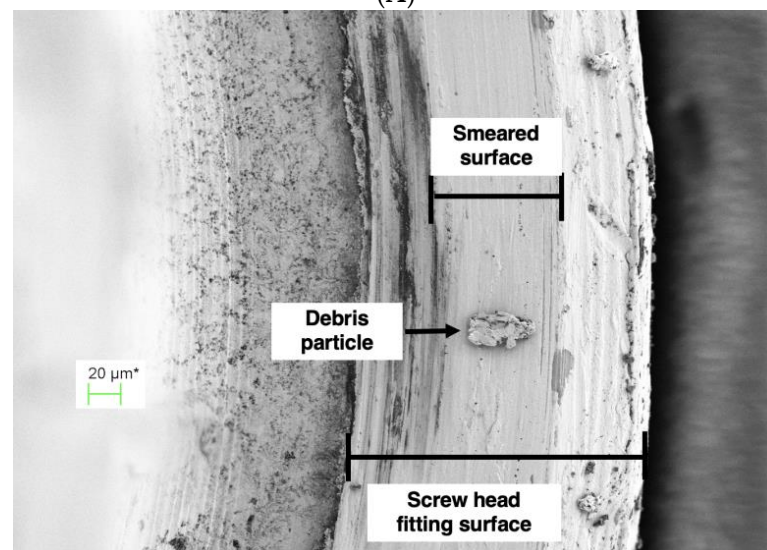
Figure 8A shows the opposing surface of the gold-plated screw head of TA PUCLA-N5 at 70× magnification. Figure 8B shows a higher magnification (563×) of part of the screw head. Again, a smeared section was evident. No bacteria were observed in the abutment cavity, indicating there was a continuous smeared region around the circumference of this screw/thread connection, resulting in an initial barrier to the *E. coli* contamination.

The abutment fitting surface in this specimen also demonstrated a smeared surface region (Figure 9A,B). If this is uninterrupted circumferentially, then it would provide a second barrier against bacterial contamination outside of the abutment. As noted previously, in this TA, the screw/thread connection provided an effective seal as there were no bacteria in the abutment space between the screw and implant connection or in the medium around the micro-gap. Therefore, it was not possible to determine if this was an uninterrupted

surface deformation at the implant/abutment connection acting as an additional effective micro-gap barrier to the screw/thread connection.



(A)



(B)

**Figure 8.** (A) Screw head fitting surface of TA PUCLA-N5 (70 $\times$ ). (B) Higher magnification (563 $\times$ ) of a section of the screw head fitting surface of TA PUCLA-N5 shows a smeared surface, which appears continuous.

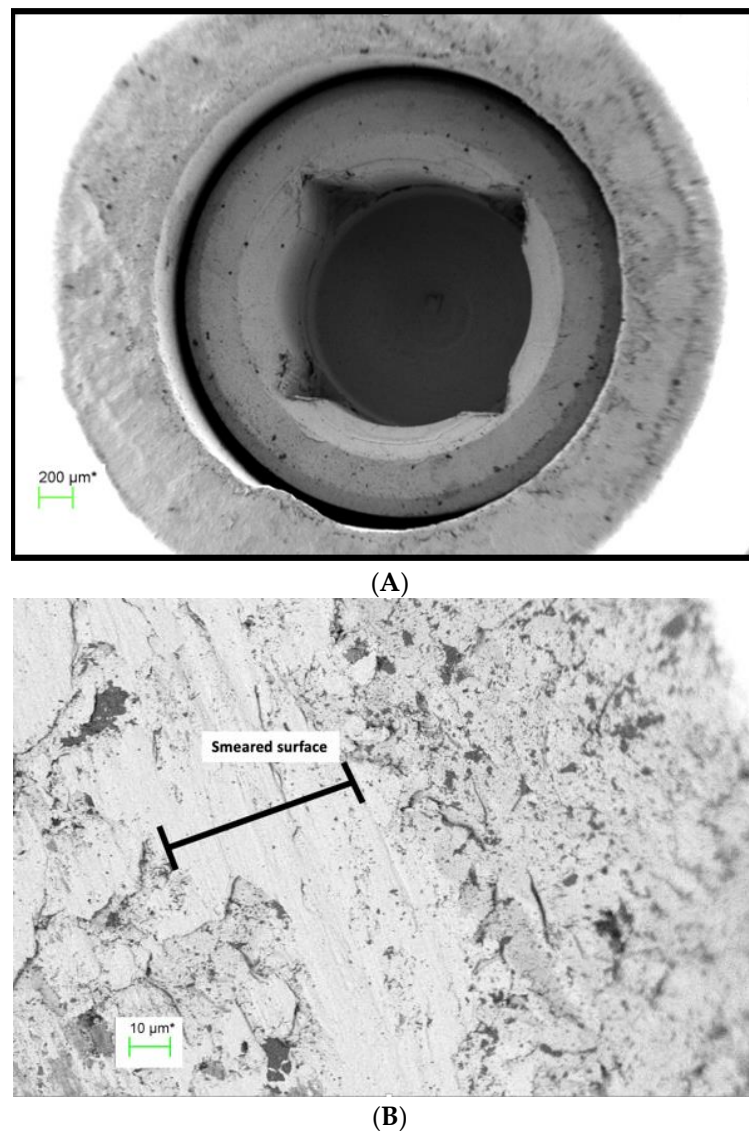


**Figure 9.** (A) Abutment fitting surface of TA PUCLA-N5 at 60× magnification showing a region of smeared surface. (B) Higher magnification of abutment fitting surface of TA PUCLA-N5 at 1580× magnification showing a region of smeared surface.

The other IACs that passed the bacterial leakage test all demonstrated bacteria in the screw chamber, indicating a lack of seal at the screw /abutment connection. Therefore, it is assumed that the smeared layer on the abutment fitting surfaces was uninterrupted around the circumference and provided the seal for *E. coli* transfer into the surrounding medium.

Contrarily, TA PUCLA-P2 failed the leakage test. There was no seal at the screw /thread connection, as evidenced by masses of bacteria in the abutment space between the abutment screw seat and abutment fitting surface (Figure 10A). There is evidence of some smearing, but this is obviously not continuous, with bacteria also evident on the outside of the abutment, possibly with remnants of the culture medium. At higher magnification, the smeared surface has the appearance of a mosaic pattern with disruptions allowing a pathway for the movement of bacteria across the micro-gap (Figure 10B).

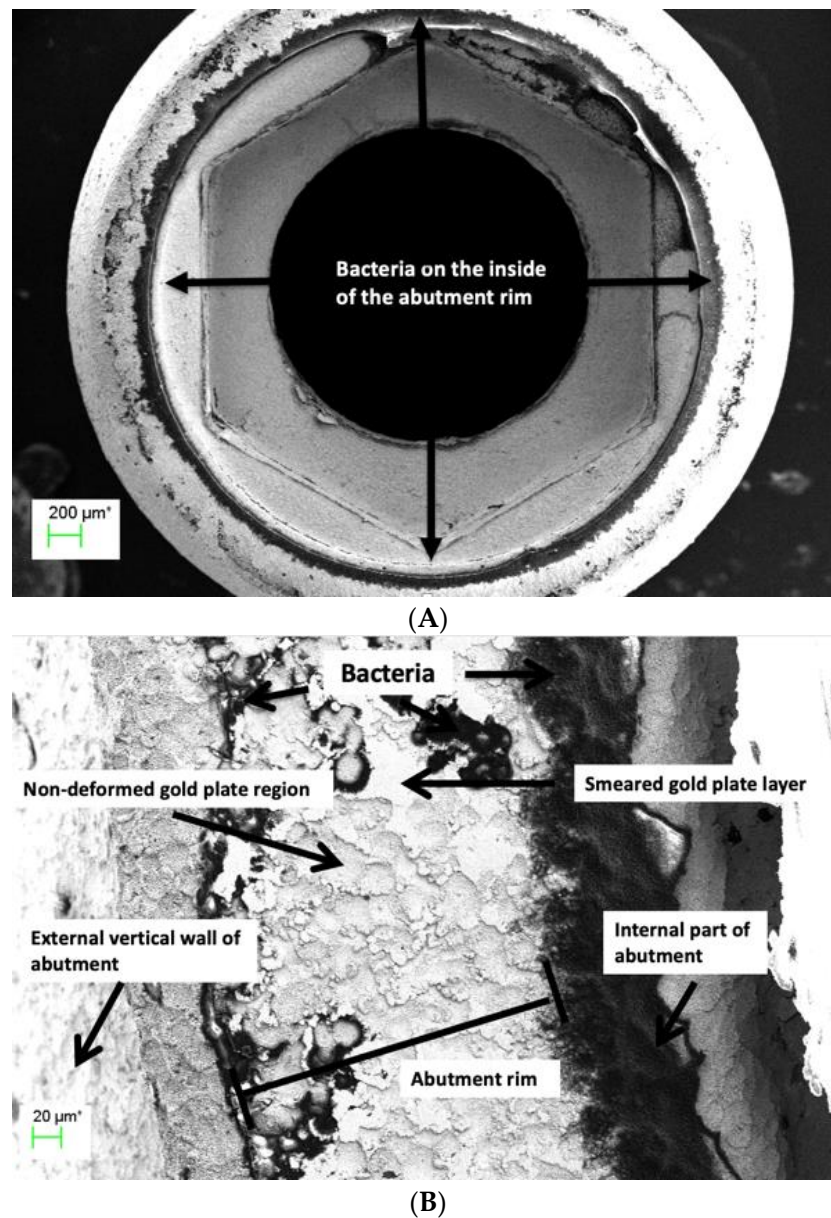


**Figure 10.** (A) Abutment rim of plated TA PUCLA-P2 at 53 $\times$  magnification. Bacteria are evident on the internal and external aspects of the abutment fitting surface. (B) Higher magnification (501 $\times$ ) of the abutment fitting surface of plated TA PUCLA-P2. Masses of bacteria are evident on the internal aspect, indicating leakage through the screw/thread connection. The smeared region shows a mosaic pattern with discontinuity across the surface and resultant bacteria on the external aspect.

#### 4. Discussion

The results of the external micro-gap measurements of the pre-machined abutments are consistent with a recent publication where the micro-gaps of both internal and external connections using pre-machined abutments were  $<2.5\ \mu\text{m}$  and confirmed that the protocols used by the commercial laboratory resulted in comparable micro-gaps to those reported in the literature [2,3]. Different methodologies and terminologies may account for the great variability in reported micro-gaps in some other studies [3]. It is apparent from the present study that micro-gap measurements at the external perimeter will vary significantly depending on the magnification and illumination used. Given the variations in surface profiles, even for machined non-plated abutments, measurements are likely to be only accurate to within  $5\ \mu\text{m}$ . However, it is difficult to reconcile the validity of biological and biomechanical effects associated with micro-gaps reported between 25

and 50  $\mu\text{m}$  and heavily cited in previous studies [10,26]. It can also be concluded that the implant-abutment connection micro-gaps of the castable UCLA abutments can be consistently less than those previously reported [4,5] and equivalent to pre-machined abutment connections. This is in agreement with the study by De Mori et al. [6], who showed that cast and machined base metal abutments showed similar gaps both after applying torque and after cyclic loading.

The micro-leakage protocol developed, including the initial sterility test, proved effective in ensuring that any bacterial transfer was confined to the screw/thread or implant/abutment connections. It can be concluded that it is possible to get an effective micro-gap barrier  $<2\ \mu\text{m}$  at the implant/abutment connection, as *E. coli* have dimensions approximately  $0.2 \times 2.0\ \mu\text{m}$  in both the castable and cast-to-UCLA abutments, with or without gold plating. However, this barrier effect was unpredictable, and the limited sample size prevented any conclusion regarding differences between the plated and non-plated cast abutments. Even if a seal is achieved at the initial implant/abutment connection, it may be broken during subsequent loading.

The SEM evaluations of the disassembled IACs demonstrated that plastic deformation (smearing) occurred at the screw/thread connection, enhancing screw preload as previously documented [16]. However, the extent of this deformation across the connections was variable and did not ensure a continuous seal. Only one of the disassembled connections examined had no bacteria in the screw shaft.

The SEM evaluations demonstrated that plastic deformation, or smearing of the abutment abutting surface, also occurred at the IAC with the high noble element content alloy and screw torque protocol used in the study. This was irrespective of whether the abutment abutting surface was gold-plated or whether it was cast or pre-machined. The non-plated abutting surfaces showed a more uniform deformation, whereas the electroplated abutting surfaces showed a more mosaic pattern. This confirms previous speculation [7] It is postulated that where these smeared regions form a continuous connection around the circumference of the abutment head, an effective seal preventing the egress of bacteria through the micro-gap is achieved. This would explain why some of the connections exhibited an effective barrier to bacterial transfer across the micro-gap, at least in the non-loaded scenario. A recently published paper demonstrated a linear relationship between gold plate deposition and plating time with the same alloy used in this study [25]. It is possible that by modifying the plating time to give a thicker Au layer, a more consistent deformation and, therefore, a more consistent bacterial barrier would be achieved on plated surfaces.

It could be argued from the results of this qualitative study that there is no benefit in gold plating the abutment implant's abutting surface. However, the high cost of gold-based alloys and new fabricating technologies, such as computer-assisted manufacturing (CAM) and 3D printing, have spurred the development of alternative abutment materials [27–29]. These alternative techniques and materials may result in increased tribocorrosion.

It has been shown that gold plating the abutments does reduce the overall volume of titanium and other elements released into the surrounding tissues, and that with cyclic loading, elemental gold is the dominant ion released [20]. Biopsy studies have shown inflammatory cells and areas of fibrosis and necrosis surrounding Ti ions in peri-implant tissues [30–32], whereas the anti-inflammatory action of gold has long been recognized in the medical field [23,24,33]. Thus, the reported zone of inflammation resulting surrounding the IAC [8] resulting from any tribocorrosion would be reduced and MBLs stabilized.

The use of gold and other noble metal coatings and nanoparticles to enhance the biocompatible and antibacterial properties of implants and abutments has been reviewed [34]. The aesthetic advantages of a golden hue have resulted in the marketing of anodized titanium abutments to create a gold luster. In addition, the resultant increase in oxygen, calcium, and phosphorus in the anodized layer may also have a positive effect on adhesion of the epithelium of the mucosal cuff [35].

Other implant and abutment surface modifications, both inorganic and organic, to induce muco-integration and shield against peri-implant diseases have also been reviewed, but many are not yet commercially available [36,37].

The deformation generated between the surfaces due to the high ductility of the gold plate may also contribute to joint stability, as occurs with the deformation of gold or teflon-coated screw surfaces [16,38], thereby contributing to the maintenance of a screw preload and reducing corrosion with dynamic loading. The influence of implant-abutment connection biomechanics and connection stability on the biological response of the peri-implant tissues has been discussed in a recent review [1].

The results of this study may explain the excellent long-term clinical outcomes of a previously published study where castable, gold-plated abutments were used [19]. Figure 11A,B show radiographs of two single implant crowns in situ for 21 years. It could be assumed that the screw seat and/or the implant/abutment interface in A have formed an effective seal against bacterial leakage through the micro-gap but not in B, possibly contributing to early marginal bone loss to the first thread.

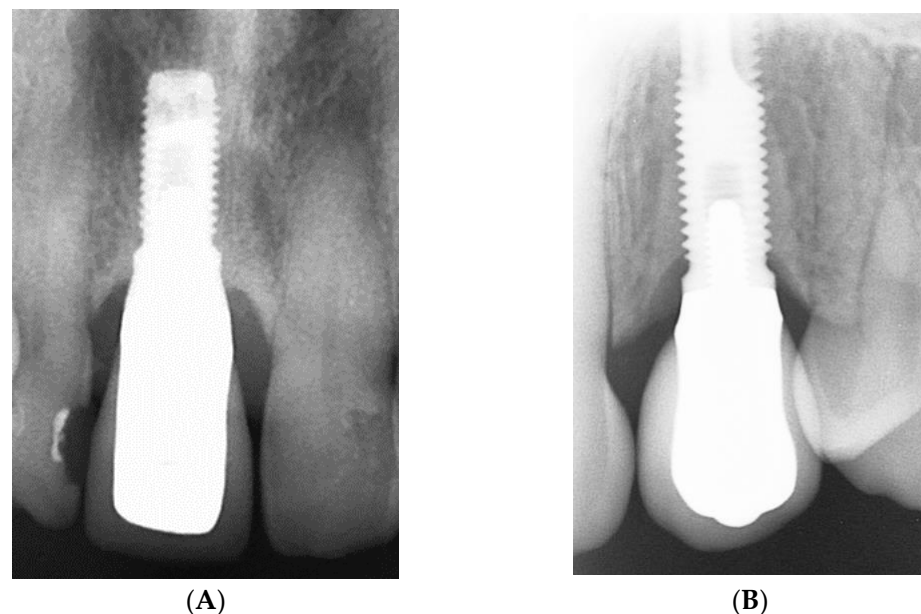


**Figure 11.** (A,B) Radiograph of single implant crowns, in situ for 21 years. In (A), there is no radiolucency at the implant/abutment interface, indicative of an effective seal at either the screw/thread or implant/abutment connections. In (B), the radiolucency extending to the first thread is indicative of a zone of inflammation resulting in loss of MBL and possibly associated with bacterial leakage through the micro-gap.

The use of gold as an abutment material has decreased significantly due to its high cost. Whether it is possible to predictably electrodeposit gold onto alternative alloys requires further research. Titanium “TiBase” abutments are commonly used in conjunction with zirconia prostheses, but titanium is not conducive to gold electrodeposition. Stainless steel may be an alternative, as stainless steel screws are currently successfully gold-plated.

The gold electrodeposit regimen employed in this study was empirically based on previous use with tooth-supported prostheses, where aesthetics, rather than any biological advantages, was the motivation for its implementation. Although it is generally accepted that machined abutments have a better fit (smaller micro-gaps) than cast abutments, the author’s published clinical results with a protocol involving cast abutments have equivalent outcomes. Therefore, the impetus for this study was to determine if the addition of the electrodeposited gold layer was a significant contributing factor. Although the limited sample size failed to indicate a definitive advantage of the gold plate, the study did

confirm that the micro-gaps of the castable UCLA abutments were equivalent to the cast-to-machined abutments.

Further research is required to ascertain if a thicker gold plate can create a more predictable seal at the IAC. Preventing the transference of *E-coli* across the micro-gap does not equate to a complete biological seal, as smaller bacteria and bacterial endotoxins may still pass across it.

The micro-gap bacterial leakage test protocol used proved effective in ensuring that any bacterial transfer was confined to the screw/abutment or implant/abutment connections. It can be concluded that it is possible to get an effective micro-gap barrier  $<2 \mu\text{m}$  at the implant/abutment connection, as *E. coli* have dimensions approximately  $0.2 \times 2.0 \mu\text{m}$  in both the castable and cast-to-UCLA abutments, with or without gold plating. However, the limited sample size prevents any conclusion regarding differences between the plated and non-plated cast abutments.

Internal abutment connections of various geometrical configurations have supplanted external hexagon connections in many regions. However, it has been documented that mechanical failures such as abutment and screw fractures are more catastrophic in internal connection systems [39]. The introduction of bi-axial implants to minimize necessity for grafting procedures has also seen a resurgence of the external hexagon design.

There are limitations to this study. Only one high-gold-content alloy and only one bacteria type were used. The test assemblies were not dynamically loaded, which may or may not enhance the plastic deformation and seal of the IACs. The limited number of test assemblies prevented a statistical analysis between the plated and non-plated test assemblies.

## 5. Conclusions

Within the limitations of the study, the following conclusions can be drawn:

1. Abutment connecting surfaces, both Au-plated and not Au-plated, showed plastic deformation (smearing) in variable mosaic patterns across the micro-gap with the high-gold-content alloys used in the study.
2. External micro-gap measurements do not give a true indication of the profiles and approximation of the abutment/implant connecting surfaces.
3. External micro-gap dimensions of cast external hexagon abutments with and without Au plating measured under shadow, eliminating silhouette illumination, averaged  $< 5 \mu\text{m}$  and were equivalent to those of the machined abutments.
4. An uninterrupted smeared layer across the abutment fitting surface can provide an effective barrier to the egress of bacteria from the internal regions of the implant.

**Funding:** This research was totally funded by the author.

**Institutional Review Board Statement:** Not applicable.

**Informed Consent Statement:** Not applicable.

**Data Availability Statement:** Data are contained within the article.

**Acknowledgments:** The author wishes to acknowledge Sarunas Petronis and Josefin Seth Caous of the SP Technical Research Institute of Sweden for their expertise in the technical operations of the SEM imaging and bacterial leakage tests.

**Conflicts of Interest:** The author declares no conflict of interest.

## Abbreviations

UCLA	University of California at Los Angeles abutments
PUCLA	Plastic castable University of California at Los Angeles abutments
GUCLA	Machined cast-to-University-of-California-at-Los-Angeles abutments
UCLA-P	University of California at Los Angeles abutments electrolytically gold-plated
UCLA-N	University of California at Los Angeles abutments not electrolytically gold-plated
IAC	Implant-abutment combinations
TA	Test assembly
MBL	Marginal bone level
SEM	Scanning electron microscope
µm	Microns
nm	Nanometres
<i>E. coli</i>	<i>Escherichia coli</i>
BHI	Brain heart infusion medium
µL	Microlitre
CAM	Computer-assisted manufacture
3D	Three dimensional

## References

- Choi, S.; Kang, Y.S.; Yeo, I.-S.L. Influence of implant-abutment connection biomechanics on biological response: A literature review of interfaces between implants and abutments of titanium and zirconia. *Prosthesis* **2023**, *5*, 527–538. [[CrossRef](#)]
- Jansen, V.K.; Conrads, G.; Richter, E.J. Microbial leakage and marginal fit of the implant-abutment interface. *Int. J. Oral Maxillofac. Implants* **1997**, *12*, 527–540.
- Vélez, J.; Peláez, J.; López-Suárez, C.; Agustín-Panadero, R.; Tobar, C.; Suárez, M.J. Influence of implant connection abutment design and screw insertion torque on implant-abutment misfit. *J. Clin. Med.* **2020**, *9*, 2365. [[CrossRef](#)] [[PubMed](#)]
- Carr, A.B.; Brunski, J.B.; Hurley, E. Effects of fabrication, finishing and polishing procedures on preload in prostheses using conventional “gold” and plastic cylinders. *Int. J. Oral Maxillofac. Implants* **1996**, *11*, 589–598.
- Byrne, D.; Houston, F.; Cleary, R.; Claffey, N. The fit of cast and machined implant abutments. *J. Prosthet. Dent.* **1998**, *80*, 184–192. [[CrossRef](#)] [[PubMed](#)]
- De Mori, R.; Ribeiro, C.F.; Neves, A.C.C. Evaluation of castable and premachined meatal base abutment/implant interfaces before and after cyclical loading. *Implant. Dent.* **2014**, *23*, 212–217. [[CrossRef](#)] [[PubMed](#)]
- Dias, E.C.L.D.C.E.M.; Bisognin, E.D.C.; Harari, N.D.; Machado, S.J.; Da Silva, C.P.; Soares, G.D.D.A.; Vidigal, G.M. Evaluation of implant-abutment microgap and bacterial leakage in five external-hex implant systems: An in vitro study. *Int. J. Oral Maxillofac. Implants* **2012**, *27*, 346–351.
- Pera, F.; Pesce, P.; Menini, M.; Fanelli, F.; Kim, B.-C.; Zhurakivska, K.; Mayer, Y.; Isola, F.; Cianciotta, G.; Crupi, A.; et al. Immediate loading full-arch rehabilitation using transmucosal tissue-level implants with different variables associated: A one-year observational study. *Dent. Oral Sc.* **2023**, *72*, 230–238. [[CrossRef](#)]
- Broggini, N.; McManus, L.; Hermann, J.; Medina, R.; Oates, T.; Schenk, R.; Buser, D.; Mellonig, J.; Cochran, D. Persistent acute inflammation at the implant-abutment interface. *J. Dent. Res.* **2003**, *82*, 232–237. [[CrossRef](#)]
- Hermann, J.S.; Cochran, D.L.; Hermann, J.S.; Buser, D.; Schenk, R.K.; Schoolfield, J.D. Biologic width around one- and two- piece titanium implants. *Clin. Oral Implants Res.* **2001**, *12*, 559–571. [[CrossRef](#)]
- Hermann, J.S.; Schoolfield, J.D.; Schenk, R.K.; Buser, D.; Cochran, D.L. Influence of the size of the microgap on crestal bone changes around titanium implants. A histomeric evaluation of unloaded non-submerged implants in the canine mandible. *J. Periodontol.* **2001**, *72*, 1372–1383. [[CrossRef](#)] [[PubMed](#)]
- King, G.N.; Hermann, J.S.; Schoolfield, J.D.; Buser, D.; Cochran, D.L. Influence of the size of the microgap on crestal bone levels in non-submerged dental implants: A radiographic study in the canine mandible. *J. Periodontol.* **2002**, *73*, 1111–1117. [[CrossRef](#)] [[PubMed](#)]
- Sahin, S.; Çehreli, M.C. The significance of passive framework fit in implant prosthodontics: Current status. *Implant. Dent.* **2001**, *10*, 85–92. [[CrossRef](#)] [[PubMed](#)]
- Albrektsson, T.; Dahlin, C.; Jemt, T.; Sennerby, L.; Turri, A.; Wennerberg, A. Is marginal bone loss around oral implants the result of a provoked foreign body reaction? *Clin. Implants Dent. Relat. Res.* **2014**, *16*, 155–165. [[CrossRef](#)] [[PubMed](#)]
- Albrektsson, T.; Jemt, T.; Mölne, J.; Tengvall, P.; Wennerberg, A. On inflammation-immunological balance theory—a critical apprehension of disease concepts around implants: Mucositis and marginal bone loss may represent normal conditions and not necessarily a state of disease. *Clin. Implants Dent. Rel. Res.* **2019**, *21*, 183–189. [[CrossRef](#)] [[PubMed](#)]
- Winkler, S.; Ring, K.; Ring, J.D.; Boberick, K.G. Implant screw mechanics and the settling effect: Overview. *J. Oral Implants* **2003**, *29*, 242–245. [[CrossRef](#)]

17. Tribst, J.P.M.; Piva, A.M.d.O.D.; da Silva-Concílio, L.R.; Ausiello, P.; Kalman, L. Influence of implant-abutment contact surfaces and prosthetic screw tightening on the stress concentration, fatigue life and microgap formation. A finite element analysis. *Oral* **2021**, *1*, 88–101. [[CrossRef](#)]
18. Sasada, Y.; Cochran, D.L. Implant-abutment connections: A review of biologic consequences and peri-implantitis implications. *Int. J. Oral Maxillofac. Implants* **2017**, *32*, 1296–1307. [[CrossRef](#)]
19. Walton, T.R. The up-to-14-year survival and complication burden of 256 TiUnite implants supporting one-piece cast abutment/metal-ceramic implant-supported single crowns. *Int. J. Oral Maxillofac. Implants* **2016**, *31*, 1349–1358. [[CrossRef](#)]
20. Silva, M.D.; Walton, T.R.; Alrabeah, G.O.; Layton, D.M.; Petridis, H. Comparison of corrosion products from implant and various gold-based abutment couplings: The effect of gold plating. *J. Oral Implantol.* **2021**, *47*, 370–379. [[CrossRef](#)]
21. Wachi, T.; Shuto, T.; Shinohara, Y.; Matono, Y.; Makihira, S. Release of titanium ions from an implant surface and their effect on cytokine production related to alveolar bone resorption. *Toxicology* **2015**, *327*, 1–9. [[CrossRef](#)] [[PubMed](#)]
22. Alrabeah, G.O.; Brett, P.; Knowles, J.C.; Petridis, H. The effect of metal ions released from different dental implant-abutment couples on osteoblast function and secretion of bone resorbing mediators. *J. Dent.* **2017**, *66*, 91–101. [[CrossRef](#)] [[PubMed](#)]
23. Yang, J.P.; Merin, J.P.; Nakano, T.; Kato, T.; Kitade, Y.; Okamoto, T. Inhibition of the DNA-binding activity of NF- $\kappa$ B by gold compounds in vitro. *FEBS Lett.* **1995**, *361*, 89–96. [[CrossRef](#)] [[PubMed](#)]
24. Zainali, K.; Danscher, G.; Jakobsen, T.; Jakobsen, S.S.; Baas, J.; Møller, P.; Bechtold, J.E.; Soballe, K. Effects of gold coating on experimental implant fixation. *J. Biomed. Mater. Res.* **2009**, *88A*, 274–280. [[CrossRef](#)] [[PubMed](#)]
25. Walton, T.R. Characterisation and electroplated gold coatings for dental applications: Estimation of thickness using non-destructive electron-probe microanalysis related to plating time. *Coatings* **2021**, *11*, 874. [[CrossRef](#)]
26. Tsuge, T.; Hagiwara, Y. Influence of lateral-oblique cyclic loading on abutment screw loosening of internal and external hexagon implants. *Dent. Mater. J.* **2009**, *28*, 373–381. [[CrossRef](#)] [[PubMed](#)]
27. Kano, S.C.; Binon, P.; Bonfante, G.; Curtis, D.A. Effect of casting procedure on screw loosening in UCLA-type abutments. *J. Prosthodont.* **2006**, *15*, 77–81. [[CrossRef](#)]
28. Øilo, M.; Nesse, H.; Lundberg, O.J.; Gjerdet, N.R. Mechanical properties of cobalt-chromium 3-unit fixed dental prostheses fabricated by casting, milling, and additive manufacturing. *J. Prosthet. Dent.* **2018**, *120*, 156.e1–156.e7. [[CrossRef](#)]
29. Presotto, A.G.C.; Cordeiro, J.M.; Presotto, J.G.C.; Rangel, E.C.; da Cruz, N.C.; Landers, R.; Barao, V.A.R.; Mesquita, M.F. Feasibility of 3D printed Co-Cr alloy for dental prostheses applications. *J. Alloys Compd.* **2021**, *862*, 158171. [[CrossRef](#)]
30. Wilson, T.G. The positive relationship between excess cement and peri-implant disease: A clinical endoscopic study. *J. Periodontol.* **2009**, *80*, 1388–1392. [[CrossRef](#)]
31. Fretwurst, T.; Buzanich, G.; Nahles, S.; Woelber, J.P.; Riesemeier, H.; Nelson, K. Metal elements in tissue with dental peri-implantitis: A pilot study. *Clin. Oral Impl. Res.* **2016**, *27*, 1178–1186. [[CrossRef](#)] [[PubMed](#)]
32. He, X.; Reichl, F.-X.; Wang, Y.; Michalke, B.; Milz, S.; Yang, Y.; Stolper, P.; Lindemaier, G.; Graw, M.; Hickel, R.; et al. Analysis of titanium and other metals in human jawbones with dental implants—A case series study. *Dent. Mater.* **2016**, *32*, 1042–1051. [[CrossRef](#)] [[PubMed](#)]
33. Jeon, K.I.; Jeong, J.Y.; Jue, D.M. Thiol-reactive metal compounds inhibit NF- $\kappa$ B activation by blocking I $\kappa$ B kinase. *J. Immunol.* **2000**, *164*, 5981–5989. [[CrossRef](#)] [[PubMed](#)]
34. Basova, T.V.; Vikulova, E.S.; Dorovskikh, S.I.; Hassan, A.; Morozova, N.B. The use of noble metal coatings and nanoparticles for the modification of medical implant materials. *Mater. Des.* **2021**, *204*, 109672. [[CrossRef](#)]
35. Traver-Mendes, V.; Camps-Font, O.; Ventura, F.; Nicolau-Sansó, M.A.; Subirà-Pifarré, C.; Figueiredo, R.; Valmaseda-Castellón, E. In-vitro characterization of an anodized surface of a dental implant collar and dental abutment on peri-implant cellular response. *Materials* **2023**, *16*, 6012. [[CrossRef](#)] [[PubMed](#)]
36. Kunrath, M.F.; Gerhardt, M.d.N. Trans mucosal platforms for dental implants: Strategies to induce muco-integration and shield peri-implant diseases. *Dental. Mater.* **2023**, *39*, 846–859. [[CrossRef](#)]
37. van Oirschot, B.A.; Zhang, Y.; Alghamdi, H.S.; Cordeiro, J.M.; Nagay, B.E.; Barao, V.A.; de Avila, E.D.; van den Beuchen, J.J. Surface engineering for dental implantology: Favoring tissue responses along the implant. *Tissue. Eng. Part A* **2022**, *28*, 555–572. [[CrossRef](#)]
38. Park, C.I.; Choe, H.C.; Chung, C.H. Effect of surface coating on the screw loosening of dental abutment screws. *Met. Mater. Int.* **2004**, *10*, 549–553. [[CrossRef](#)]
39. Yi, Y.; Koak, J.-Y.; Kim, S.-K.; Lee, S.-J.; Heo, S.-J. Comparison of implant component fractures in external and internal type: A 12-year retrospective study. *J. Adv. Prosthodont.* **2018**, *10*, 155–162. [[CrossRef](#)]

**Disclaimer/Publisher’s Note:** The statements, opinions and data contained in all publications are solely those of the individual author(s) and contributor(s) and not of MDPI and/or the editor(s). MDPI and/or the editor(s) disclaim responsibility for any injury to people or property resulting from any ideas, methods, instructions or products referred to in the content.